Excitable Waves and Spatiotemporal Patterns in a Fixed-Bed Reactor

Martin Barto and Moshe Sheintuch
Dept. of Chemical Engineering, Technion-Israel Institute of Technology, Haifa 32000, Israel

Spatiotemporal patterns existing in a one-dimensional fixed-bed reactor with oscillatory or excitable kinetics are analyzed to develop the methodology of motion identification and classification. The reactor model accounts for a local (solid-phase) oscillator and a global (gas-phase) convective interaction. The local oscillator incorporates a fast and diffusing surface temperature and a localized activity as its dynamic variables. Such kinetics admit a traveling pulse solution or homogeneous oscillations in a uniform medium. In a fixed-bed reactor, the local conditions in the bed (the phase plane character) vary along the system. The response of an excitable bed to local perturbations depends on its location (at inlet or outlet) and the nature of the initial steady state (ignite or extinguished). The main spatiotemporal-sustained patterns in the bed are: almost homogeneous oscillations that appear as parallel bands in the time-space contour map; oscillatory fronts that emerge from the reactor exit, and aperiodic motion that appears as split-bands. Pattern selection is determined by the phase planes spanned by the reactor and the ratio of the two slowest time scales: front residence time and period of oscillations.

Introduction

Extensive investigation into catalytic oscillations (Razon and Schmitz, 1987) revealed a large class of reactions that admit this behavior. Recent effort is focusing on spatiotemporal patterns and a plethora of such patterns were reported for one-dimensional catalytic ribbons and wires. These include antiphase temperature oscillations during methylamin decomposition on an electrically heated Rh wire (Cordonier et al., 1989); two temperature pulses moving in opposite directions from a point on a Pt wire during ammonia oxidation (Cordonier and Schmidt, 1989); back-and-forth temperature pulses on a controlled Pt ribbon catalyzing propylene oxidation (Phillippou et al., 1991) and a moving temperature pulse on a Ni ring during hydrogen oxidation in a CSTR (Lane and Luss, 1992). Antiphase oscillations and moving pulses of current density were recorded during the anodic dissolution of a Ni wire in sulfuric acid under galvanostatic or potentiostatic conditions, respectively (Lev et al., 1990).

The patterns reported above for high-pressure catalytic reactions are different from those encountered in liquid-phase reacting systems (for example, the Belousov-Zhabotinski reaction, see Field and Burger, 1985) or in physiological systems like the heart muscle and eye retina (Winfree, 1987). Motions in these and other chemical oscillators include target patterns, spiral waves and standing waves. Such two-dimensional patterns of adsorbed species were observed by Ertl (1991) on a single isothermal platinum crystal catalyzing the low pressure oxidation of carbon monoxide. Such patterns are unlikely to appear in high-pressure catalytic oscillators since due to the high exothermicity the temperature is the fast autocatalytic variable and thermal conduction usually favors homogeneity of solutions. The patterns observed at high pressures were induced, in some cases, by external control or by gas-phase interaction.

While catalytic wires, rings and disks are simple one- and two-dimensional model systems that lend themselves to comparison with theory, the working-horse of the catalytic process is the fixed bed. The purpose of this work is to analyze qualitatively and quantitatively spatiotemporal patterns which may arise in a one-dimensional fixed-bed reactor with oscillatory or excitable kinetics in order to develop the methodology for motion identification and classification. This analysis will en-

Current address of M. Barto: Laboratory of Reaction Engineering, Slovak Technical University, Radlinskeho 9, 812 37 Bratislava, Czechoslovakia.

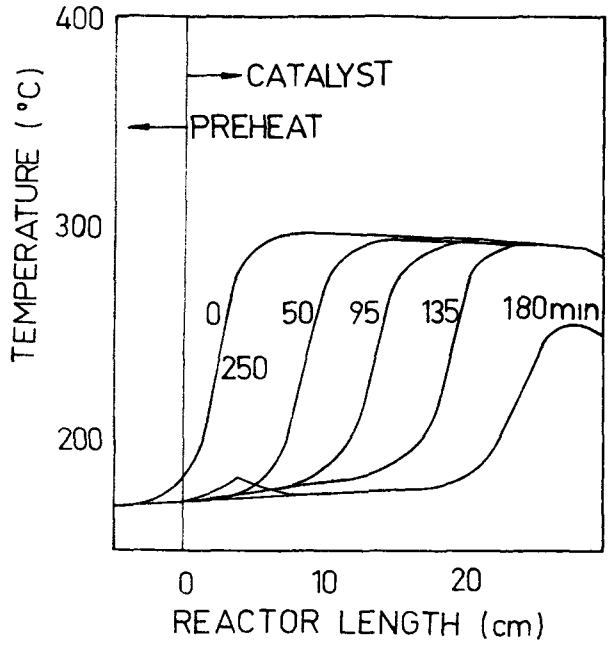

Figure 1. Excitable waves observed during ethylene oxidation by air in a Pt/Al_2O_3 bed.

Feed flow was 200 cm^3/min, and it was preheated in a 20-cm preheating section and a 5-cm adiabatic section packed with glass beads. $T_{fin} = 443$ K, $c_{fin} = 1.1\%$ vol.

able predicting possible characteristic motions in the reactor and implement necessary adjustments or control of reactor operating conditions. The motions in the fixed-bed reactor differ from those in a uniform medium due to the convective flow and the effects of reactor boundaries: the local conditions in the bed (fluid concentration and temperature) vary in conjunction with the state of the system and the local state of a single pellet (that is, the corresponding phase-plane) may vary from an excitable one, upstream, to an oscillatory one, downstream.

This work is motivated by the observation by Sheintuch and Adjaye (1990) of excitable waves during ethylene oxidation in a (30 cm long) bed packed with (3.2 mm cylindrical 0.5%) Pt/Al_2O_3 catalytic pellets. Setting a local perturbation at the inlet (Figure 1) induced a front that moved at constant speed and shape. The front always moved downstream until its exit. A hot spot appeared then at the inlet (at 180 min, Figure 1), it developed and spread across the reactor and the old steady state was established. This motion is different from other known transients in a fixed-bed, like solutions in which the system decays towards its steady state along the time-space characteristics (Fiolitakis et al., 1979) or from fronts that creep and move upstream or downstream towards the final steady state (Rhee et al., 1974; Simon and Vortmeyer, 1978). The latter motions occur in response to a step change in operating conditions and the system ends up in a new steady state. Fixed-bed transients were reviewed by Hlavacek and van Rompay (1981).

The structure of this article is the following: in the next section we introduce the reactor model which accounts for a local (solid-phase) oscillator and a global (gas-phase) convective interaction. The local oscillator incorporate a fast and diffusing surface temperature and a localized (nondiffusing) activity as its dynamic variables. Such kinetics induce excitable or oscillatory behavior in a uniform medium and the regions of excitability and oscillations are adjacent in the phase-plane. We also review the qualitative theory of excitable waves in a uniform medium, as well as in a packed bed, and present original simulations of such waves to corroborate the analysis. In the third section, we present periodic and aperiodic motions and analyze their relation to the phase-plane behavior.

Qualitative Analysis and Excitable Motions

Excitable medium is a spatially extended system resting in a stable steady state which is susceptible to destabilization by a perturbation. Imposing a local perturbation in a uniform distributed system creates a pulse traveling with asymptotically constant velocity and shape; when the perturbed state is unique then the original state is recovered after the pulse exists. This motion is accounted for by a model that incorporates a fast and diffusing autocatalytic variable and a slow and localized inhibitor. This structure is met in catalytic thermal oscillations, which are believed to be caused by coupling of thermal multiplicity, due to enthalpy acceleration, together with a slow and reversible change in surface activity; the latter may be caused by poisoning, catalyst oxidation and reduction or surface rearrangement.

The solid phase enthalpy balance, which can be written in the form,

$$\tau_T \frac{\partial T}{\partial t} - L_T^2 \cdot \frac{\partial^2 T}{\partial x^2}$$

$$= \frac{(-\Delta H) \cdot r(T, \phi, c_A) \cdot \rho_b}{h A_v} - (T - T_f) \equiv F_1(T, \phi, c_A; T_f) \quad (1)$$

$$\left. \frac{\partial T}{\partial x} \right|_{x=0,L} = 0$$

accounts for accumulation, conduction, heat generation and heat-removal; it is subject to no-flux boundary conditions at its ends. The conduction length scale and thermal time scale are defined as

$$L_T = \sqrt{\frac{\lambda}{h \cdot A_v}}$$

$$\tau_T = \frac{(\rho c_p)_s \cdot (1 - \epsilon)}{h \cdot A_V}$$

We justify now our choice of parameters and estimate the values of these scales. There are only few empirical correlations for fixed-bed thermal conductivity (λ) in the literature (for example, Votruba et al., 1972) and for alumina packed beds this value is of order of O(1 J/m·s·K), (see Eigenberger, 1972). Empirical correlations for heat (h) and mass-transfer (k_g) coefficients are abundant (Froment and Bischoff, 1990), and we chose values similar to those in Eigenberger (1972). The solid phase heat capacity $(\rho c_p)_s$ was also adopted from the latter reference. We then find L_T to be typically of $O(10^{-3}$ cm) for packed beds. When a front solution exists its width is of $O(L_T)$

and it is therefore much shorter than the bed length. The time scale of the solid phase is $O(10^{-1}$ s) and is much shorter than that associated with either conduction or surface modification. Thus, when a front develops, it travels at a speed of L_T/τ_T (0.01 cm/s) and it takes about 1,000–10,000 s to travel at 10–100-cm-long reactor (compare Figure 1).

The local mass balance accounts for accumulation, reaction and mass transfer:

$$\tau_c \frac{\partial c_A}{\partial t} = -\frac{r(T, \phi, c_A)\cdot\rho_b}{k_g A_v} - (c_A - c_{Af}) \equiv F_2(c_A, T, \phi; c_{Af}) \quad (2)$$

The diffusion term is ignored since interpellet interaction occurs through the gas phase. The time scale associated with changes in concentration

$$\tau_c = \frac{(1-\epsilon)}{k_g A_v}$$

is similar to τ_T in order of magnitude. The reaction rate is assumed to follow first-order Arrhenius kinetics, and the rate is proportional to the fraction of active surface (ϕ):

$$r = k_w c_A \exp\left(\frac{-E}{R\cdot T}\right)\cdot\phi$$

Equations 1 and 2 are the fast subset of the local dynamics; since $c_A(T, \phi)$ from $F_2 = 0$ is monotonic we can substitute it into $F_1 = 0$ to obtain the autocatalytic nullcurve:

$$F(T, \phi; c_{Af}, T_f) = \frac{(-\Delta H)\cdot k_g \cdot c_{Af}\cdot\rho_b}{h} \cdot \frac{k_W \cdot \exp\left(\frac{-E}{R\cdot T}\right)\cdot\phi}{\left[k_W \cdot \exp\left(\frac{-E}{R\cdot T}\right)\cdot\phi\cdot\rho_b + k_g A_v\right]} - (T - T_f) = 0 \quad (3)$$

The first term on the righthand side is simply the heat generation function, and it is written as a product of the adiabatic temperature rise and the sigmoidal kinetic function.

The surface modification process is slow and nondiffusive and is described, for simplicity, by a dependence of the form

$$\frac{d\phi}{dt} = G(T, \phi) = -(k_d^- + \mu\cdot(T - T_{\text{fin}}))\cdot\phi + (k_d^+ - \mu\cdot(T - T_{\text{fin}}))\cdot(1-\phi) \quad (4)$$

so that $G = 0$ is a straight line in the phase plane, that is expressed as

$$T - T_{\text{fin}} = \frac{-k_d^-\cdot\phi + k_d^+\cdot(1-\phi)}{\mu}$$

and is independent of c_{Af} or T_f. The nature of $G(T, \phi)$ is important only in determining the type of local dynamics. The system admits oscillatory solution with periods of $O(1/k_d)$. Experimentally the observed periods are in the range 100–1,000 s.

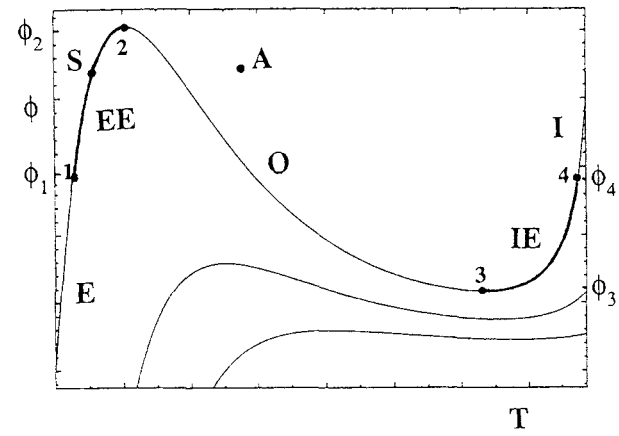

Figure 2. Analysis of motions in the phase plane.

Three $F(T, \phi; T_f) = 0$ curves with different T_f values (the intersection with $f = 0$) are shown and the domains of characteristic behavior are denoted.

We start by reviewing the local dynamics of relaxation oscillations and excitability. If the operating conditions (c_{Af}, T_f) are uniform throughout the bed, and $\tau_T \ll 1/k_d$ the dynamics is determined by the curve $F = 0$ and Eq. 4. Suppose that $F = 0$ is S-shaped (that is, due to thermal bistability) and that a unique steady state (the intersection of $F = 0$ and $G = 0$) exists. If the steady state is located on the unstable portion of $F = 0$, then the system exhibits relaxation oscillations, undergoing deactivation along the ignited branch of $F = 0$, followed by a slow activation along the extinguished branch. If the stable state lies on the upper or lower branch of $F = 0$, then the steady state is stable, but the system may be excitable; a sufficiently large perturbation (for example, from S to A, Figure 2) results in a long excursion, along the opposite branch of $F = 0$, before the original steady state is reestablished. Perturbations should be sufficiently large to cross the unstable branch and, thus, smaller perturbations are required to excite a system lying near the limit points of $F = 0$ (points 2 and 3, Figure 2).

In an extended one-dimensional medium, communicating by heat conduction and exposed to uniform operating conditions, such a local perturbation at the edge will trigger a front that propagates towards the other edge while the temperature of the perturbed edge relaxes along $F = 0$. Eventually, another transition will occur and an opposite front will form. These fronts will propagate through the system until their exit at the other edge. The bed relaxes then to its original steady state. The front velocity depends on the fluid temperature and the catalyst activity spanned by it. For a sufficiently narrow front, a certain velocity can be assigned for each ϕ. This varies from a positive value near ignition, that is, when the ignited section is expanding, to a negative value at the extinction point. In between, there exists a set of stationary fronts (for example, for $\phi_1 = \phi_4$, Figure 2). The leading front described above, propagating by conduction, is called a *trigger front*. The relaxation fronts often propagate due to local ignition or extinction (the system reaches the limit point of $F = 0$ before the front arrives) and such a wave is called a *phase wave*. If the activity gradient is small, the phase wave velocity exceeds that of a trigger front.

The main modification to the picture drawn above, in describing the motion in a fixed bed, is due to changing operating conditions. The fluid-phase balance is usually established rap-

idly in comparison with either front motion or deactivation in the bed. Fluid-phase axial dispersion terms were ignored since they are not expected to change the structure of solution; note that fluid temperature and concentration are continuous and the corresponding dispersion effects across the front are expected to be small in comparison with heat conduction through the solid phase. Radial gradients of temperature and concentration are assumed negligible. The fluid phase enthalpy balance then is:

$$\tau_{Tf}\cdot\frac{\partial T_f}{\partial t}=-v\cdot\tau_{Tf}\cdot\frac{\partial T_f}{\partial x}-(T_f-T) \tag{5}$$

where the convective time scale associated with the changes of fluid temperature

$$\tau_{Tf}=\frac{\epsilon\cdot(\rho c_p)_f}{hA_v}=\tau_T\cdot\frac{\epsilon\cdot(\rho c_p)_f}{(1-\epsilon)\cdot(\rho c_p)_s}$$

is $O(10^{-2}$ s) and v is 0.1-1. m/s in order of magnitude. The fluid phase mass balance is

$$\tau_{cf}\cdot\frac{\partial c_{Af}}{\partial t}=-v\cdot\tau_{cf}\cdot\frac{\partial c_{Af}}{\partial x}-(c_{Af}-c_A) \tag{6}$$

and the corresponding convective time scale

$$\tau_{cf}=\frac{\epsilon}{k_g A_v}=\tau_c\cdot\frac{\epsilon}{(1-\epsilon)}$$

is of $O(10^{-1}$ s). Fluid phase balances are subjected to the inlet conditions:

$$x=0:\quad c_{Af}=c_{\mathrm{Afin}};\quad T_f=T_{\mathrm{fin}} \tag{7}$$

Numerical simulations of the model were performed by a finite difference scheme with 100 equidistant mesh points. The resulting set of ordinary differential equations with a small parameter was solved using a semi-implicit Runge-Kutta method of the fourth order with the band matrix solver. The solid temperature profiles were presented as colored contours in the plane of time vs. position in the reactor (the presented figures are black and white pictures of original colored plates and the

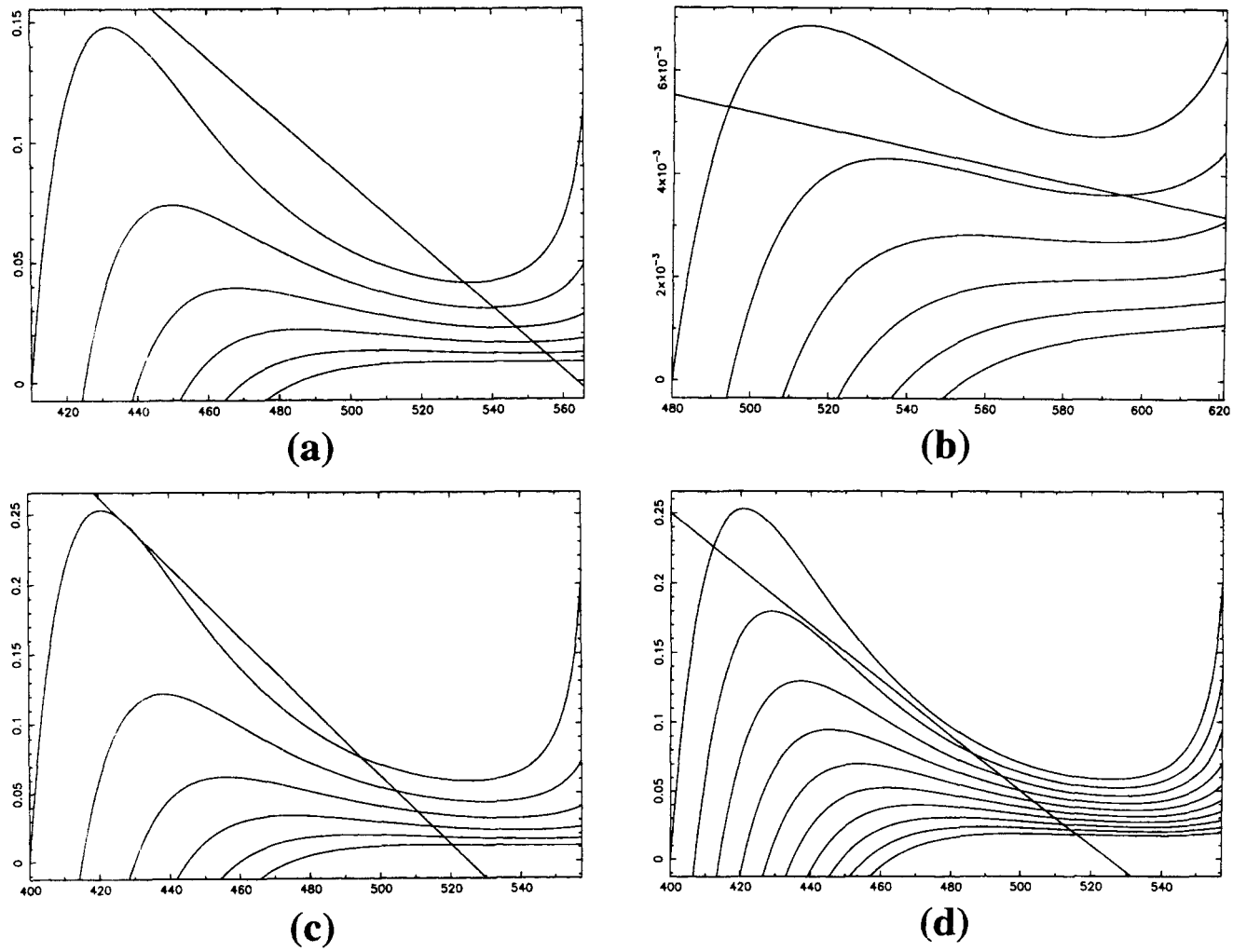

Figure 3. Family of nullcurves $F=0$ and line $G=0$ for typical situations in Figure 6a, 8b, 10c, and 11d.

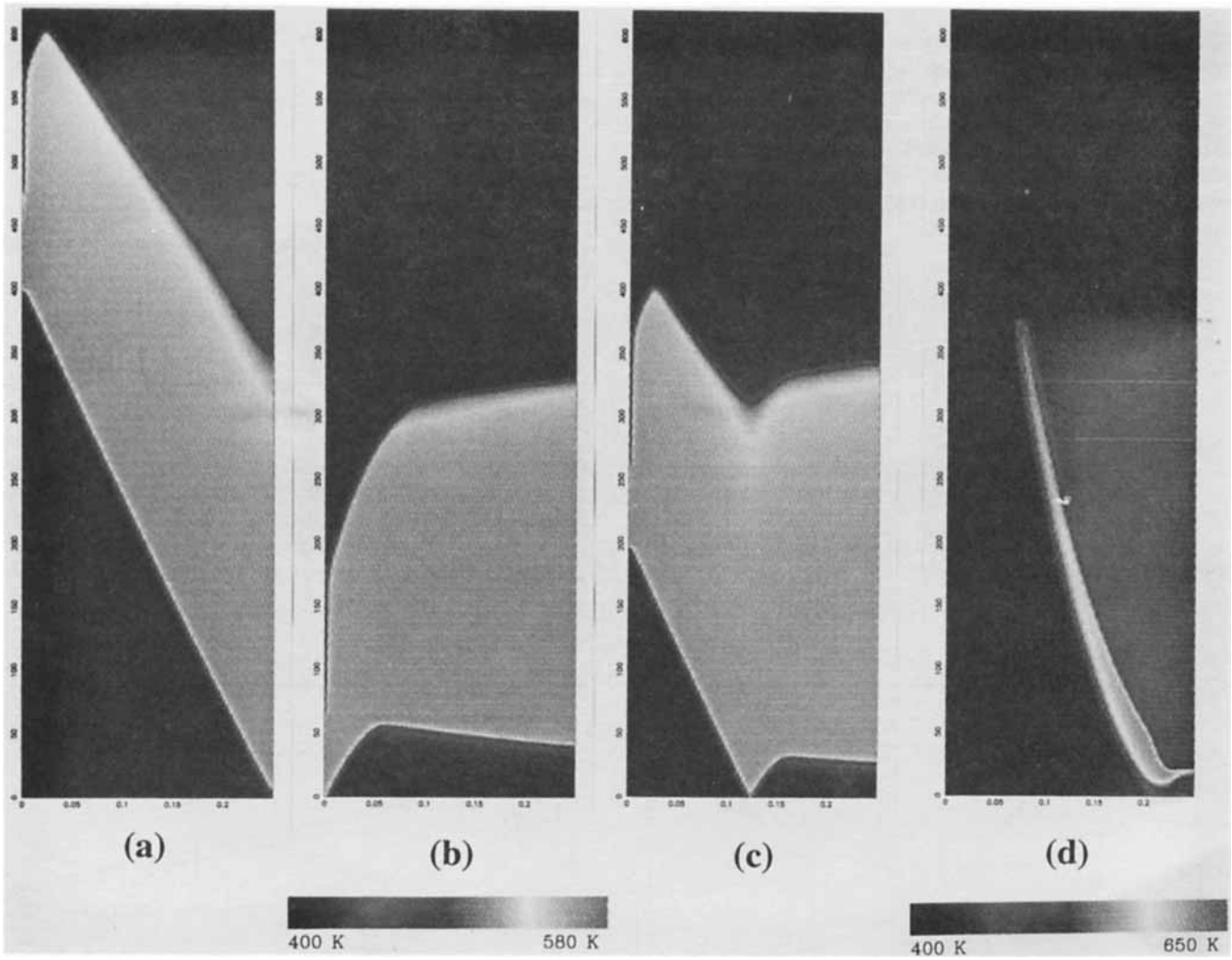

Figure 4. Ignition fronts in an excitable bed induced by a perturbation.

Perturbation applied at the outlet (a), at the inlet (b), or at the center of the reactor (c): $k_d^- = 1 \times 10^{-3}\ s^{-1}$, $k_d^+ = 4 \times 10^{-3}\ s^{-1}$, $\mu = 1.67 \times 10^{-5}\ (K \cdot s)^{-1}$, $L = 25$ cm, $T_{fin} = 400$ K; a pulse created at the outlet of a reactor that spans E and EE regions (d): $k_d^- = 1 \times 10^{-3}\ s^{-1}$, $k_d^+ = 9 \times 10^{-3}\ s^{-1}$, $\mu = 1.1 \times 10^{-5}\ (K \cdot s)^{-1}$, $L = 25$ cm, $T_{fin} = 400$ K. (Results are presented in the time-space plane with t varying form 0 to 600.)

temperature is shown as a gray scale; the fronts are the sharp interphases between the light (ignited) and dark (extinguished) zones in the reactor). The values of physiochemical constants and model parameters which were employed in the simulations are summarized in the Appendix.

To present the motion in the phase-phase we plot a family of nullcurves $F = 0$ and the straight line $G = 0$ (Figures 2 and 3). The curves $F = 0$ are parametrized by the fluid temperature, which is the temperature at $\phi = 0$ (that is intersection with the abcissa). Fluid temperature and concentration are related by a pseudo-steady-state approximation. The system may span one or several of the following regions: extinguished state (E) (with steady state at $\phi < \phi_1$), extinguished excitable (EE) ($\phi_1 < \phi < \phi_2$ on the low temperature branch), oscillatory (O), ignited excitable (IE) ($\phi_3 < \phi < \phi_4$ on the upper branch) and ignited state (I) ($\phi > \phi_4$). While we can determine the motion at the inlet, the outlet behavior and the zones spanned by the reactor are determined by the kinetics and the reactor length. The motion may also span domains with three solutions in which the two extreme ones are either both unstable (that is, on the intermediate branch, we refer to this phase plane as O_3) or both stable (M) or one stable and one unstable (U_3).

Excitable fronts occur when the reactor spans at steady state the regions EE or IE but does not span the O region. In that case, the motion includes front(s) created by a perturbation followed by relaxation front(s). Typical situations are described in qualitative terms and are illustrated by corroborating computations:

1. If the inlet lies in the EE regions then, in a sufficiently short reactor, the outlet belongs to the same section. Excitations may be applied to any point of the reactor.

(a) If an ignition front is created at the outlet then it will move upstream; the domain upstream is not affected by this motion and the front shape and velocity changes only slightly due to the space-dependence of the fluid concentration and temperature profiles at steady state (Figure 4a). The fluid temperature downstream from the front increases as the solid phase is ignited and the activity declines along the ignited branch. The ensuing extinction front is most likely to appear at the outlet, the point with the longest residence in the ignited state.

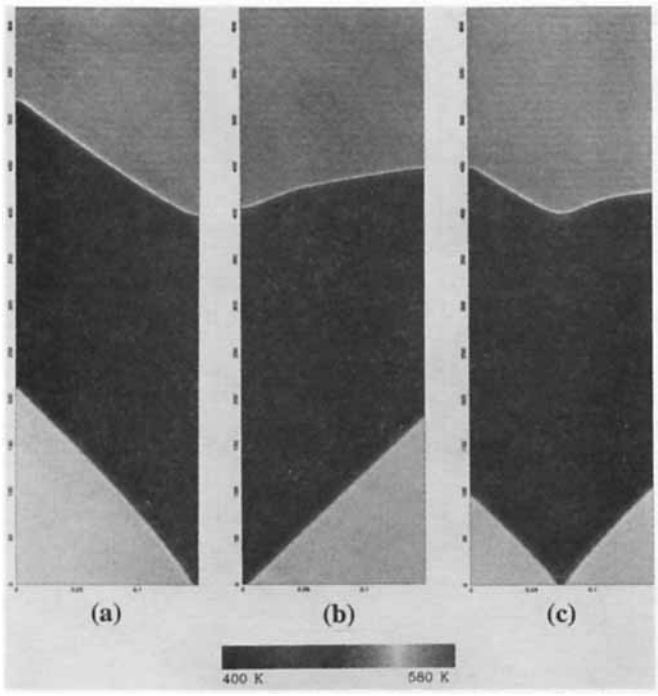

Figure 5. Extinction fronts in an excitable bed induced by a perturbation.

Perturbation applied at the outlet (a); at the inlet (b); or at the center of the reactor (c): $k_d^- = 1 \times 10^{-3}\ s^{-1}$, $k_d^+ = 1.5 \times 10^{-3}\ s^{-1}$, $\mu = 6.2 \times 10^{-6}\ (K \cdot s)^{-1}$, $L = 15$ cm, $T_{fin} = 400$ K. (Results are presented in the time-space plane with t varying form 0 to 600.)

This front does not affect conditions upstream but the upstream section deactivates slowly. The relaxation front is likely to be a phase front with a velocity that is almost identical to that of the first front. To show that note that when the initial front has passed a certain position the activity jumps to its initial position-independent high value and then it decays to the limit point. The limit point temperature varies weakly with fluid temperature, but since this is a steady solution in a moving coordinate then T_f at the second front position is time-independent, as long as the first front is within the reactor.

(b) When an ignition is created at the inlet then the expanding ignited zone increases the fluid temperature downstream, inducing an ignition front at the outlet which propagates as a phase wave (Figure 4b). The following relaxation by an extinction front occurs at the inlet, and for most of its voyage, it propagates as a phase front since the information is transmitted downstream via the fluid phase.

(c) When excitation is applied to any point within the reactor then the two ignition fronts, one moving upstream and another downstream, behave as described earlier- as trigger and phase fronts, respectively (Figure 4c). The front moving upstream, however, accelerates the motion of the downstream-moving front, since the fluid temperature in the bed increases.

2. If the inlet lies in the *IE* region then the outlet will belong either to the *IE* or *I* region.

(a) Since reaction along the ignited branch is fast then the outlet is excitable only in a sufficiently short reactor. An extinction front moving from the reactor outlet does not affect upstream section; in a short reactor the temperature does not vary significantly along the bed and the front velocity is almost unchanged (Figure 5a). The relaxation ignition front moves at a similar velocity for the reasons described in case 1a.

(b) Extinction front starting from the inlet has a constant velocity, since the conditions at the front are similar to those at the inlet and are almost time-independent (Figure 5b). The relaxation to the original steady state occurs via an ignition front that is transmitted by the gas phase in similarity to the case 1b. Note the similarity to Figure 1.

(c) Perturbation of any point within the reactor generates two trigger fronts that move in opposite directions and then subsequently two relaxation fronts. These fronts behave along the principles described above (Figure 5c).

3. If the reactor inlet is unexcitable but its exit is located on the excitable branch (*EE*) then excitation of the outlet generates trigger and relaxation fronts in similarity to case 1a above. The traveling pulse slows down when it approaches the conditions corresponding to a stationary front. Deactivation leads then to the decay of the pulse and its disappearance (Figure 4d).

Oscillatory Behavior

If some part of the reactor belongs to the *O* region, at least within a certain part of the cycle, then we should expect spontaneous generation of fronts. The fronts may originate at any point in the reactor, and they interact in a manner similar to that explained for excitable fronts. The dominant pace center is expected to be the point with the highest frequency as it imposes its frequency and prevails. The fronts sent from the fastest pace center are annihilated with those originated at the slower center. This annihilation point will move towards the slower pacer in the next cycles and eventually will conquer it. However, if the inlet belongs to the excitable section it will not serve as a pace center, but it may still oscillate due to front propagation. If the inlet belongs to a stable unexcitable branch then upstream propagating fronts slow down until they come to a halt and die out by changing activity in similarity to the motion in Figure 4d.

As the model discussion illustrates, there are two slow steps in the process: front propagation time, which is $\tau_T L/L_T$ in order of magnitude, and deactivation time; other rates are much faster in most actual situations. In the following simulations, the slow time scales are comparable; their ratio vary with the reactor length which is chosen as the bifurcation variable in most simulations. The reactor length affects also the dynamics spanned by the reactor.

If the inlet is oscillatory and the reactor is not too long, then the outlet belongs to the same section and is likely to become the pace center, as its frequency is the highest due to the higher fluid temperature and the smaller activity amplitude (see phase plane—Figure 3a). The system exhibits then almost homogeneous oscillations that appear as parallel bands. Note that the boundaries of the ignited and extinguished zones move fast, and they are phase fronts for most of the cycle except in the vicinity of the inlet (Figure 6a). To understand the fact note that within the extinguished branch the fluid temperature does not climb significantly above that of the inlet and ignition is likely to occur everywhere simultaneously. The residence along the ignited state is weakly dependent on fluid temperature, and extinction occurs again almost simultaneously. In a sufficient long reactor, the extinction front may be generated at

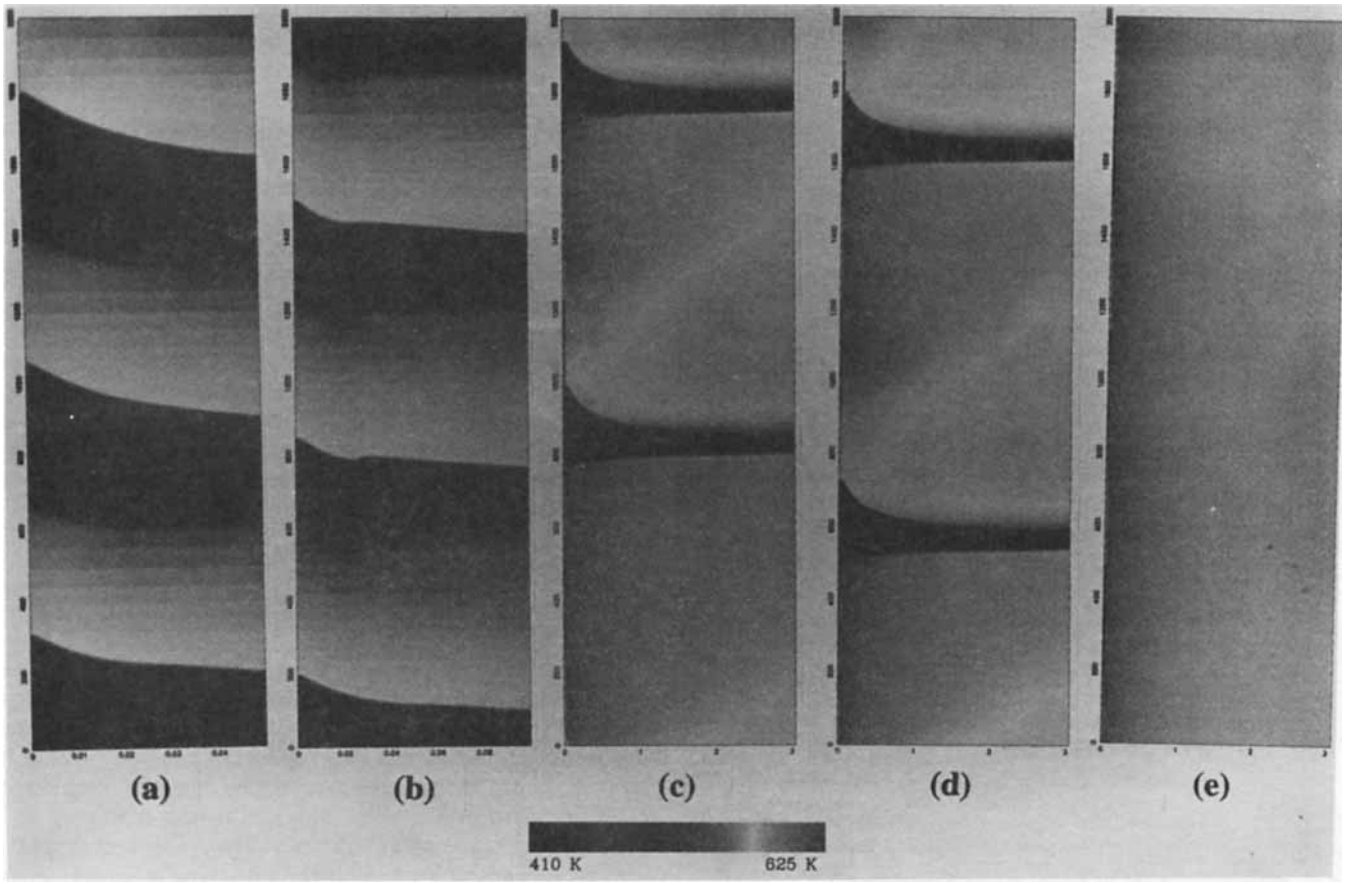

Figure 6. Periodic, almost homogeneous, spatiotemporal patterns in a reactor that spans O-IE-I regions.

(a) $L = 5$ cm; (b) $L = 10$ cm; (c) $L = 302$ cm; (d) $L = 305$ cm; (e) $L = 307$ cm: $k_d = 1 \times 10^{-3}$ s^{-1}, $k_d^* = 4 \times 10^{-3}$ s^{-1}, $\mu = 6.5 \times 10^{-6}$ (K·s)$^{-1}$, $T_{fin} = 410$ K. (Results are presented in the time-space plane with t varying form 0 to 2,000.)

some point inside the reactor (Figure 6b) or even at the inlet (Figure 6c). Very long reactors exhibit long periods (Figures 6c and 6d) in which the system is ignited for most of the cycle. Increasing reactor length from 305 cm to 307 cm leads to a hard bifurcation (probably through infinite-period transition) into a stable ignited state (Figure 6e).

If the inlet is excitable (that is, it belongs to *EE* section), then in a sufficiently long reactor a periodic regime develops in the outlet. In a reactor of length just above the bifurcation point to oscillatory solution, the fronts are generated at the reactor outlet (Figure 7a, $L = 5$ cm); the downstream section of the reactor oscillates almost homogeneously while the information is transmitted to the inlet zone, which is excitable, via slow trigger fronts. A snapshot of temperature profile in the reactor may show two or three upstream-moving pulses and an almost homogeneous tail. Prolonging the reactor causes the pace center for both ignition and extinction fronts to move inwards (Figure 7b and 7c), but the structure of a homogeneous zone and a pulse zone is maintained. A fine structure develops now and the point of pulse disappearance varies from one cycle to another showing period two, three or four oscillations (that is, the point of disappearance repeats itself after two, three or four cycles; Figures 7b–7d). Further increase in the reactor length causes the fine structure to disappear as the downstream section moves out of the oscillatory region into the stable one. The outlet oscillates with a small amplitude in response to changes of fluid temperature caused by the oscillations inside the reactor (Figure 7e).

If the inlet is extinguished and unexcitable (E), then again there exists a critical bifurcation reactor length (L^*) so that oscillations develop for longer reactors. The simulations show that there is a global bifurcation when L crosses a certain critical value ($L^* = 16.24$ cm in Figure 8a): An oscillatory front motion suddenly emerges from the reactor outlet. An ignited zone is formed and expands until the front reaches its stationary position; slow deactivation changes it then to an extinction front and the ignited zone shrinks and disappears. The frequency changes only slightly when changing the reactor length. For this set of parameters, there exists a domain of fluid temperatures for which the local dynamics is bistable (M, Figure 3b). With increasing length, the hot zone penetrates deeper into the reactor but in a sufficiently long reactor a stationary front emerges (Figure 8b).

In another set of parameters with a *E-EE-O* sequence of phase planes, we simulated quasiperiodic front motion (Figure 9). The slowly modulating frequency disappears when the small parameter which represents the ratio of the rate of the catalytic activity changes to reaction rate (that is, k_{d-}/k_W) is increased. The transition to these patterns is similar to that described above.

For a set of parameters for which there exist three unstable solutions at the inlet (O_3, see phase portrait in the Figure 3c),

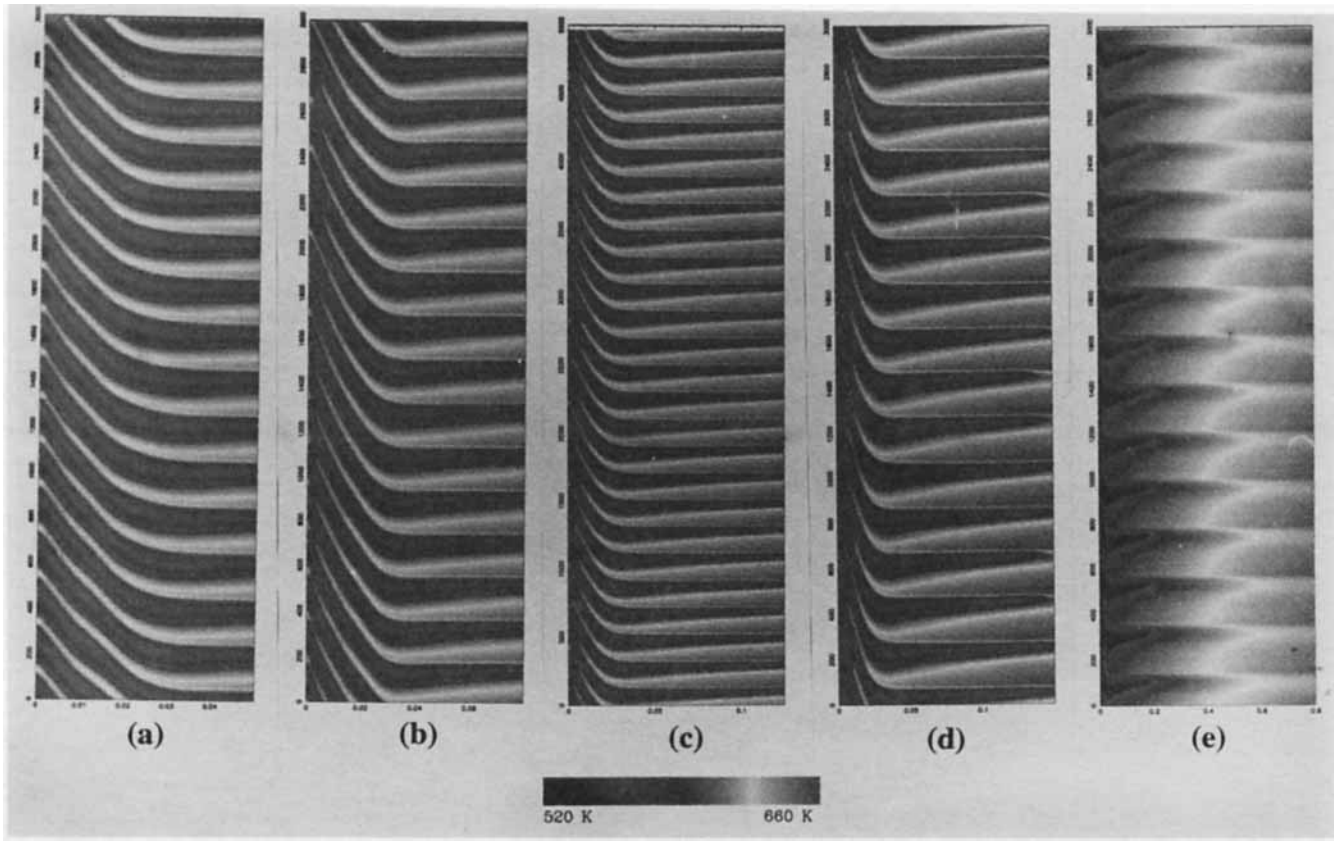

Figure 7. Spatiotemporal multiperiodic patterns in a reactor spanning EE-O-IE-I regions.

(a) $L = 5$ cm; (b) $L = 8$ cm; (c) $L = 12.5$ cm; (d) $L = 15$ cm; (e) $L = 80$ cm: $k_d^- = 4 \times 10^{-5}$ s^{-1}, $k_d^+ = 2 \times 10^{-2}$ s^{-1}, $\mu = 1.24 \times 10^{-7}$ (K·s)$^{-1}$, $T_{fin} = 520$ K. (Results are presented in the time-space plane with t varying form 0 to 3,000.)

we find a new behavior in which a wide pulse creates a narrow one in its wake (Figure 10a). We refer to it as *split-band*. The long time presentation of this behavior is shown in Figure 10b using an approximate model which traces the front position by an approximate expression for the front velocity (Sheintuch, 1990). The narrow pulses are short-lived, and they decay or disappear by coalescence with other bands. Changing the parameters in a way that eliminates the multiplicity at the inlet causes the pattern to change into a regular periodic one (similar to Figure 6a).

Split-band appear also when the inlet is unique and excitable (region *EE*), but the reactor spans domains with multiple solutions (O_1, see Figure 3d for the corresponding phase portrait). The solution is periodic for short reactor and band splitting appears beyond a critical reactor length (see Figures 11a-11c).

Discussion and Conclusions

The simulated motions in a fixed bed with local oscillatory or excitable kinetics are different than those known for an open one-dimensional system with uniform ambient (gas-phase) conditions: Under the assumed properties of the model, which incorporates a fast and diffusive autocatalytic variable and a localized slow variable, the uniform system admits homogeneous oscillations, with oscillatory kinetics, or a propagating pulse solution induced by a local perturbation of an excitable state. While a traveling pulse in a uniform media may be created by perturbation of the ignited or extinguished state at either the left or right edge, the response of the bed to such a perturbation depends on its position and the initial state. The main sustained spatiotemporal patterns in the bed appear as parallel bands, oscillatory fronts and split-bands. Parallel bands appear when the bed spans an oscillatory domain: In a sufficiently short reactor, the oscillations are almost homogeneous and the bands are almost horizontal. If the inlet is excitable and extinguished, the bands bend towards the inlet (Figure 5), and several upstream-moving pulses may appear in the reactor; their interaction with the oscillatory backstream section may lead to aperiodicity. If the inlet is unexcitable, the bands terminate short of the inlet. Oscillatory fronts appear in a long reactor when the inlet is unexcitable. Split-bands were shown to be associated with the existence of an O_3 or U_3 zone in the reactor, and the aperiodicity is induced by the interaction of the upstream- and downstream sections. Pattern selection is determined, therefore, by the phase planes spanned by the reactor and the ratio of the two slowest time scales: front residence time and oscillations period. Splitting of propagating pulses has been recently reported to exist in a one-dimensional excitable medium of the Belousov-Zhabotinski reaction (Sevcikiva et al., 1992) and in low-pressure CO oxidation on Pt(110) (Bar et al., 1992). When the reactor, or part of it, spans the bistability domain a stationary front solution may be reached (Figure 8b).

The next natural step of this research would be to extend

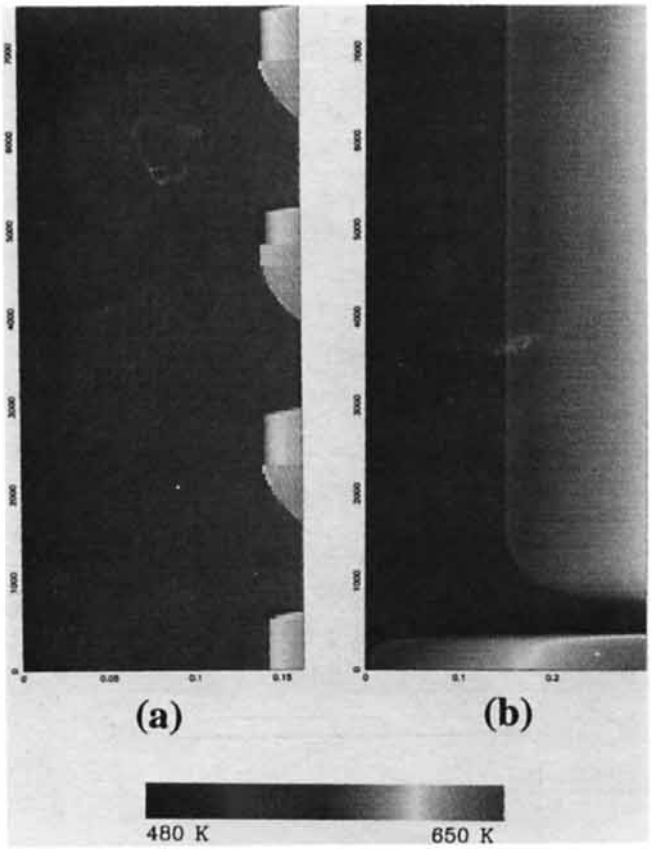

Figure 8. Oscillatory fronts simulated in a reactor spanning the E-EE-O-M-IE-I regions.

(a) $L = 16.24$ cm; (b) $L = 30$ cm: $k_d^- = 2 \times 10^{-5}$ s^{-1}, $k_d^+ = 3.6 \times 10^{-3}$ s^{-1}, $\mu = 6 \times 10^{-8}$ (K·s)$^{-1}$, $T_{fin} = 480$ K. (Results are presented in the time-space plane with t varying form 0 to 7,000.)

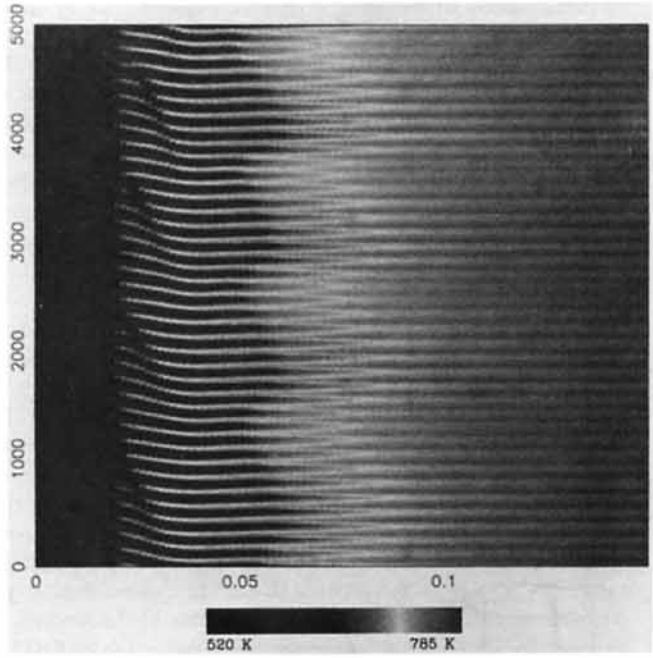

Figure 9. Quasiperiodic patterns simulated in a reactor spanning the E-EE-O-IE-I regions.

$k_d^- = 2 \times 10^{-5}$ s^{-1}, $k_d^+ = 5 \times 10^{-2}$ s^{-1}, $\mu = 6.2 \times 10^{-8}$ (K·s)$^{-1}$, $T_{fin} = 520$ K.

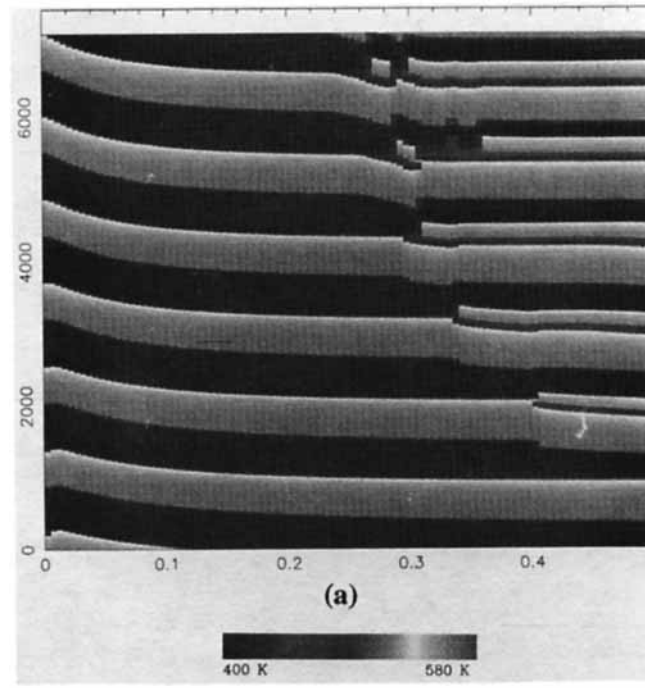

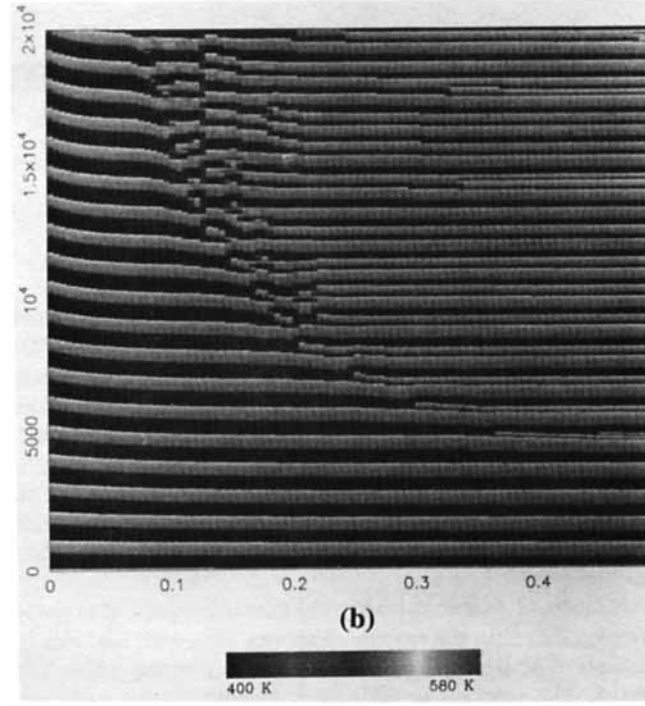

Figure 10. Split-band pattern in a reactor spanning the O_3-O-IE regions.

Simulation of (a) original model (Eqs. 1-7) and (b) approximate solution: $k_d^- = 1 \times 10^{-3}$ s^{-1}, $k_d^+ = 2.2 \times 10^{-3}$ s^{-1}, $\mu = 8.2 \times 10^{-6}$ (K·s)$^{-1}$, $T_{fin} = 400$ K.

the analysis to two- and three-dimensional patterns. Patterns on a uniform plane or disk include target- patterns and spiral waves while scroll waves are possible in three dimensions. Note that a thin slice of the bed, when exposed to a uniform feed, should behave like a disk and exhibit such patterns. The pattern or its properties may vary along the bed and a certain spatial organization will emerge. The simulation of such complex mo-

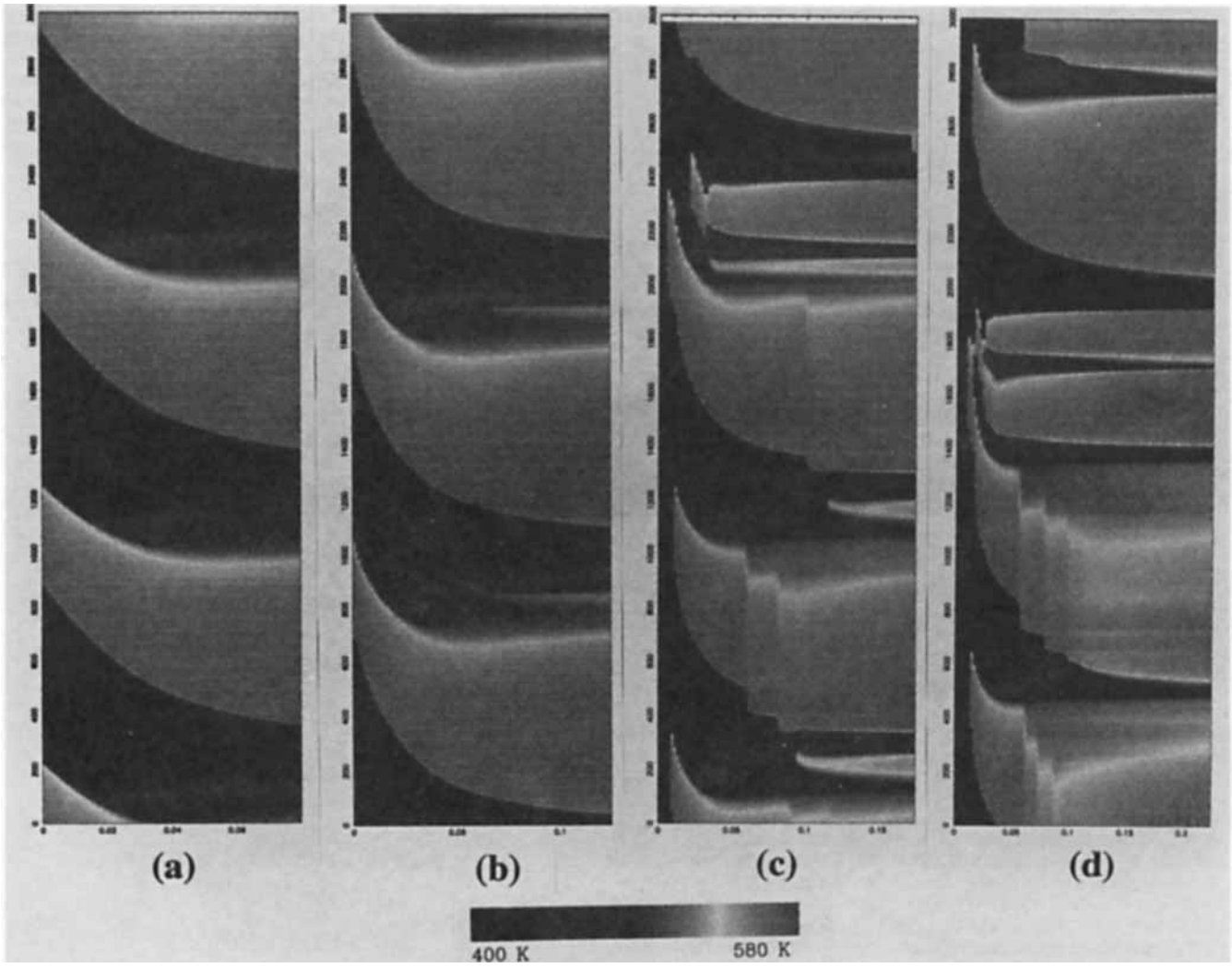

Figure 11. Split-band pattern in a reactor spanning the EE-E-O_3-IE regions.

(a) $L = 8$ cm; (b) $L = 12$ cm; (c) $L = 17.5$ cm; (d) $L = 22.5$ cm: $k_d^- = 1 \times 10^{-3}$ s^{-1}, $k_d^+ = 3 \times 10^{-3}$ s^{-1}, $\mu = 8 \times 10^{-6}$ (K·s)$^{-1}$, $T_{fin} = 400$ K. (Results are presented in the time-space plane with t varying form 0 to 3,000.)

tions is beyond our computer means and will require certain numerical approximations or model simplifications that will be presented elsewhere.

Acknowledgment

Work was supported by the U.S.-Israel Binational Science Foundation. Financial support provided by the Planning and Budget Committee of the Israel Council for Higher Education to Martin Barto is highly appreciated.

Notation

A_v = interphase surface area per reactor volume
c_A = key component concentration
c_p = specific heat capacity
E = activation energy of the catalytic reaction
h = heat-transfer coefficient
ΔH = reaction enthalpy
k_g = mass-transfer coefficient
k_w = catalytic reaction rate constant
L = reactor length
L_T = conduction length scale
R = gas constant
t = time
T, T_f = solid and fluid temperature, respectively
v = fluid velocity
x = axial coordinate

Greek letters

ϵ = bed void fraction
λ = bed thermal conductivity
μ = coefficient of the temperature dependence of activation/deactivation
ρ = density
ρ_b = bed density
τ_c = characteristic time of the solid concentration changes
τ_{cf} = characteristic time of the fluid concentration changes
τ_T = characteristic time of the solid temperature changes
τ_{Tf} = characteristic time of the fluid temperature changes
ϕ = activity

Subscripts

f = fluid phase
in = inlet

s = solid phase
$\bullet$ = bifurcation value

Superscripts

0 = initial conditions
$\bullet$ = bifurcation value

Literature Cited

Adjaye, J., and M. Sheintuch, "Comparison of Multiplicity Patterns of a Single Catalyst Pellet and a Fixed Catalytic Bed for Ethylene Oxidation," *Chem. Eng. Sci.*, **45**, 1331 (1990).

Bar, M., M. Eiswirth, H. H. Rotermund, and G. Ertl, "Solitary Wave Phenomena in an Excitable Surface Reaction," *Phys. Rev. Lett.*, **69**, 945 (1992).

Cordonier, G. A., F. Schuth, and L. D. Schmidt, "Oscillations in Methylamine Decomposition on Pt, Rh and Ir: Experiments and Models," *J. Chem. Phys.*, **91**, 5374 (1989).

Cordonier, G. A., and L. D. Schmidt, "Thermal Waves in NH_3 Oxidation on a Pt Wire," *Chem. Eng. Sci.*, **44**, 1983 (1989).

Eigenberger, G., "On the Dynamic Behavior of the Catatlytic Fixed-Bed Reactor in the Region of Multiple Steady States—1. The Influence of Heat Conduction in Two Phase Models," *Chem. Eng. Sci.*, **27**, 1909 (1972).

Ertl, G., "Oscillatory Kinetics and Spatio-Temporal Self-Organization in Reactions at Solid Surfaces," *Sci.*, **254**, 1750 (1991).

Field, R. J., and M. Burger, *Oscillations and Travelling Waves in Chemical Systems*, John Wiley, New York (1985).

Fiolitakis, E., U. Hoffmann, and H. Hoffman, "Investigation of Reaction Kinetics by Wavefront Analysis," *Chem. Eng. Sci.*, **34**, 677 (1979).

Froment, G., and K. B. Bischoff, *Chemical Reactor Analysis and Design*, 2nd ed., John Wiley, New York (1990).

Hlavacek, V., and P. van Rompay, "Current Problems of Multiplicity, Stability and Sensitivity of States in Chemically Reacting Systems," *Chem. Eng. Sci.*, **36**, 1587 (1981).

Lane, S., and D. Luss, personal communication (1992).

Lev, O., M. Sheintuch, G. Yarnitzky, and L. Pismen, "Spatial Current Distribution During Nickel Anodic Dissolution in Sulfuric Acid," *Chem. Eng. Sci.*, **45**, 839 (1990).

Philippou, G., F. Schulz, and D. Luss, "Spatiotemporal Temperature Patterns on an Electrically Heated Ribbon," *J. Chem. Phys.*, **95**, 3224 (1991).

Razon, L. F., and R. A. Schmitz, "Multiplicities and Instability in Chemically Reacting Systems—A Review," *Chem. Eng. Sci.*, **42**, 1005 (1984).

Rhee, H., R. P. Lewis, and N. R. Amundson, "Creeping Profiles in Catalytic Fixed Bed Reactors. Continuous Models," *Ind. Eng. Fundam.*, **42**, 317 (1974).

Ševičiková, H., M. Marek, and S. C. Müller, "The Reversal and Splitting of Waves in an Excitable Medium Caused by an Electrical Field," *Sci.*, **257**, 951 (1992).

Sheintuch, M., "Numerical Approaches for Computation of Fronts," *Numerical Methods for Partial Differential Equations*, **6**, 43 (1990).

Sheintuch, M., and J. Adjaye, "Excitable Waves in a Fixed Bed Reactor: Ethylene Oxidation on Platinum," *Chem. Eng. Sci.*, **45**, 1897 (1990).

Simon, B., and D. Vortmeyer, "Measured and Calculated Migration Speeds of Reaction Zones in Fixed Bed Reactor: A Quantitative Comparison," *Chem. Eng. Sci.*, **33**, 109 (1978).

Votruba, J., V. Hlavacek, and M. Marek, "Packed Bed Axial Thermal Conductivity," *Chem. Eng. Sci.*, **27**, 1845 (1972).

Winfree, P. T., *When Time Breaks Down*, Princeton University Press, Princeton, NJ (1987).

Appendix

Parameters employed in all simulations were:

$$(-\Delta H) = 2.84 \times 10^5 \text{ J/(mol·K)}$$

$$C_{A\text{fin}} = 3 \text{ mol·m}^{-3}$$

$$k_g A_v = 6.825 \times 10^1 \text{ s}^{-1}$$

$$k_w \rho_b = 4.51 \times 10^{11} \text{ s}^{-1}$$

$$E = 8.1 \times 10^4 \text{ J/(mol·K)}$$

$$hA_v = 3.49 \times 10^5 \text{ J/(m}^3\text{·K·s)}$$

$$\epsilon = 0.35$$

$$\lambda = 1 \text{ J/(m·s·K)}$$

$$(\rho c_p)_f = 1.17 \times 10^3 \text{ J/(m}^3\text{·K)}$$

$$(\rho c_p)_s = 7.88 \times 10^5 \text{ J/(m}^3\text{·K)}$$

$$v = 3 \text{ m/s}$$

Manuscript received Dec. 28, 1992, and revision received Mar. 9, 1993.